

ARVO 2025 presentations on Imagine Eyes' AO retinal imaging

Click on the title to find the abstract in this document.

Times in CET

rtx1™ Adaptive Optics Retinal Camera

POSTER session: High Resolution Imaging and Clinical Applications

Sun, May 4 | 3:15pm - 5:00pm

- ***Pigment redistribution in and at the border of GA lesions***
Morphometric analysis of the near-infrared hypo-reflective clumps associated with late-stage AMD in Flood Illumination Adaptive Optics (FIAO)
Evelyn Markle (University of Pittsburgh, USA)
Poster #A0130

POSTER session: Retinitis pigmentosa and IRD I

Mon, May 5 | 8:30am - 10:15am

- ***Rtx1 AO camera reveals cone mosaic alteration in pre-symptomatic RP with normal BCVA***
Deep phenotyping of PRPF31-associated Dominant Retinitis Pigmentosa
Kirk Stephenson (Hospital for Sick Children, Toronto, CA)
Poster #A0017

POSTER session: Adaptive optics, microscopy, MRI, ultrasound, and other imaging technologies

Mon, May 5 | 3:00pm - 4:45pm

- ***New AI-assisted analysis of cone photoreceptor density on rtx1 AO montages***
The Influence of Image Quality on Cone Density Measurements in Adaptive Optics Flood Illumination Ophthalmoscopy
Danilo Andrade De Jesus (Erasmus MC, Rotterdam, NL)
Poster #A0060

POSTER session: Retinitis pigmentosa and IRD II

Tue, May 6 | 8:30am - 10:15am

- In-depth phenotypic study of a Novel Autosomal Dominant RPE65-related Retinal Dystrophy
Filip Van den Broeck (Ghent University Hospital, BE)
Poster #B0158
- ***rtx1 cone density metric detects RP progression over a 4x shorter timescale than OCT***
A two-year prospective natural history study of EYS-associated retinitis pigmentosa (KEYS study): assessment of progression using OCT and adaptive optics
Kiyoko Gocho (15-20 National Eye Hospital, FR; Kobe Eye Center, JP)
Poster #B0171
- ***More sensitive assessment of RP progression with cone density than visual function outcomes***
Correlation Between Cone Density and Visual Function in 27 EYS-RP Patients Using AO Fundus Camera: A Subset Analysis of the KEYS Study
Masakazu Hiraoka (Kobe Eye Center, JP)
Poster #B0199

Morphometric analysis of the near-infrared hypo-reflective clumps associated with late-stage AMD in Flood Illumination Adaptive Optics (FIAO)

Abstract 1005 - Poster A0130

Evelyn Markle^{*1,2}, Valerie C. Snyder¹, Min Zhang¹, Yse Borella^{3,4}, Kunal K. Dansingani¹, Joseph N. Martel¹, Jay Chhablani¹, Jose Alain Sahel¹, Ethan A. Rossi¹

¹Department of Ophthalmology, University of Pittsburgh, Pittsburgh, Pennsylvania, United States; ²Department of Neuroscience, University of Pittsburgh, Pittsburgh, Pennsylvania, United States; ³Hopital National des 15-20, Paris, Île-de-France, France; ⁴Sorbonne Universite, Paris, Île-de-France, France

Disclosures: Evelyn Markle: Code N (No Commercial Relationship) | Valerie C. Snyder: Code N (No Commercial Relationship) | Min Zhang: Code N (No Commercial Relationship) | Yse Borella: Code N (No Commercial Relationship) | Kunal K. Dansingani: Code N (No Commercial Relationship) | Joseph N. Martel: Code N (No Commercial Relationship) | Jay Chhablani: Code N (No Commercial Relationship) | Jose Alain Sahel: Code N (No Commercial Relationship) | Ethan A. Rossi: Code N (No Commercial Relationship)

Purpose

Hypo-reflective clumps (HRCs) are structures associated with geographic atrophy (GA) in AMD. Originally identified with flood-illumination adaptive optics (FIAO), HRCs have been hypothesized to be macrophages that have accumulated RPE organelles, including melanin, via the phagocytosis of debris from atrophied RPE. We recently showed in a small sample of GA lesions that most HRCs are autofluorescent (AF) in the near infrared (NIR), consistent with the hypothesis that they contain melanin. Here, we examined HRCs in a large number of GA lesions to understand how their morphometry and topography vary across a range of lesion sizes.

Methods

17 eyes of 12 patients (mean age: 73) with GA and HRCs, previously imaged with FIAO, were evaluated. GA lesions were segmented manually and then dilated by 50 μm to include any HRCs on the border of the GA. HRCs were then segmented using a threshold-based approach. Finally, lesion and HRC properties were quantified using MATLAB. Lesion area, diameter, and shape properties were quantified. HRC quantification included HRC count, area, major/minor axes, diameter, Feret's aspect ratio, and density.

Results

36 GA lesions were evaluated. Mean lesion area was 0.361 mm^2 (range: 0.083-1.52 mm^2). 3,000 HRCs were segmented. Mean HRC area was 364.3 μm^2 (SD: 475 μm^2). Mean HRC diameter was 21.14 μm (SD: 14.1 μm). Overlapping HRCs were often segmented as a single HRC, causing the size distributions to be skewed with a long tail representing overlapping HRCs. Mean Feret's aspect ratio was 1.66 (SD: 0.67), showing that most HRCs were elliptical. Mean HRC density was 244.27 (SD: 53.1). Lesion area was correlated with the number of HRCs within each lesion ($R^2=0.87$).

Conclusions

HRC morphology was similar across all lesions, at least for individual HRCs. This consistency in HRC size across many GA lesions of varying sizes strengthens the hypothesis that they are of a common cellular origin. Interestingly, despite some variability, HRC density was mostly consistent across the lesion sizes examined here. Future studies should evaluate the regional distribution of HRCs in larger lesions where HRCs may be distributed less uniformly. Ongoing longitudinal study of HRC dynamics will provide insight into the evolution of HRCs and their relation to GA progression.

Deep phenotyping of PRPF31-associated Dominant Retinitis Pigmentosa

Abstract 1444 – Poster A0017

Kirk A.J. Stephenson^{*1}, **Brian Ballios**^{3,2}, **Elise Heon**¹, **Ajoy Vincent**¹

¹Department of Ophthalmology & Vision Sciences, The Hospital for Sick Children, Toronto, Ontario, Canada; ²Department of Ophthalmology & Visual Sciences, Kensington Vision and Research Centre, Toronto, Ontario, Canada; ³Department of Ophthalmology & Visual Sciences, University Health Network, Toronto, Ontario, Canada

Disclosures: Kirk A.J. Stephenson: Foundation Fighting Blindness: Code F (Financial Support): none | Brian Ballios: Code N (No Commercial Relationship) | Elise Heon: Deep Genomics: Code C (Consultant/Contractor): none; Editas: Code C (Consultant/Contractor): none; Fighting Blindness Canada: Code F (Financial Support): none; Janssen: Code C (Consultant/Contractor): none; Novartis: Code C (Consultant/Contractor): none | Ajoy Vincent: Code N (No Commercial Relationship)

Purpose

To clinically characterize the structural and functional ophthalmic features in *PRPF31*-mediated dominant retinitis pigmentosa (RP).

Methods

The study was approved by the Research Ethics Board of The Hospital for Sick Children & adhered to tenets of the Declaration of Helsinki. Subjects with a (likely) pathogenic variant in *PRPF31* & RP features were included after providing informed consent. All participants had detailed examination, axial length measurement, multimodal retinal imaging (MMI), & flood illumination adaptive optics [AO (rtx1, Imagine Eyes, France)] imaging. Cone mosaic was analysed in a semi-automated fashion at 2° temporal to the fovea. Cone mosaic data (cone density [CD], cone spacing [CS]) was contrasted with best corrected visual acuity (BCVA), Goldmann visual fields (GVF) III4e isopter horizontal diameter & other MMI features (optical coherence tomography [OCT] horizontal ellipsoid zone [EZ] width & central retinal thickness [CRT]). Findings were contrasted between children, parents and controls.

Results

Eight participants met the inclusion criteria (age 12 – 59 years, 63% female) including 3 parent-child pairs (2/3 parents were ‘asymptomatic’ but had RP features). Mean BCVA was 0.20 ±0.30 LogMAR, with 88% ≤0.3 LogMAR. Mean III4e horizontal diameter (84.4 ±46.7°) was less than normal (130°, p<.001). CD & CS at 2° temporal to the fovea were not associated with any GVF parameters.

Mean spherical equivalent refraction was +0.41 ±1.73D. EZ width was significantly less than controls (4484 ±2952 vs 7870 ±262, p=.014). Cone mosaic significantly deviated from normative values for CD (16656 ±4890 vs 28884 cones/mm², p<.001) & CS (8.95 ±2.07 vs 6.49µm, p<.001). Neither CD (r²=0.006, p=.772) nor CS (r²=0.097, p=.087) were linearly associated with age.

Although parents & children had differing peripheral measures, including CRT^{3-6mm} (265 ±13 vs 232 ±25µm, p=.009), parents were indistinguishable from their affected children for CRT^{1mm} (p=.168), CD (19284 ±2491 vs 18021 ±2325 cones/mm², p=.556) and CS (8.00 ±0.55 vs 8.30 ±0.56, p=.502).

Conclusions

PRPF31-RP shows highly variable expressivity though all subjects in this study showed signs of RP. Abnormalities in the central cone mosaic were identified even in pre-symptomatic disease where measures such as BCVA were normal. Cone mosaic assessment by AO may be useful as an anatomical outcome measure (with functional extrapolations) for future therapies targeting *PRPF31*-RP.

Layman Abstract (optional): Provide a 50-200 word description of your work that non-scientists can understand. Describe the big picture and the implications of your findings, not the study itself and the associated details.

PRPF31-associated retinitis pigmentosa (RP) classically exhibits incomplete penetrance. We investigated both symptomatic patients and ‘carrier’ parents using a variety of functional and structural tests. Visual acuity was within the normal range in 88% and myopia was not a strong feature, differing from other forms of RP. We found that even asymptomatic ‘carriers’ had reduced cone density and increased cone spacing to a level similar to their children. Measurement of the cone mosaic may be a sensitive outcome measure for future therapeutic trials.

The Influence of Image Quality on Cone Density Measurements in Adaptive Optics Flood Illumination Ophthalmoscopy

Abstract 1962 - Poster A0060

Danilo Andrade De Jesus^{*1,2}, *David Green*³, *Darren Hargreaves*³, *Jane Gray*³, *Neda Shahedy*⁶, *Marine Durand*⁴, *Nicolas Chateau*⁴, *Sebastiaan Koninkx*¹, *Pam Heutinck*¹, *Kübra Liman*¹, *Caroline C W Klaver*^{1,5}, *Theo van Walsum*¹, *Alberta Thiadens*¹, *Panos Sergouniotis*^{3,6}, *Luisa Sanchez Brea*¹

¹Erasmus MC, Rotterdam, ZH, Netherlands; ²Oogziekenhuis Rotterdam, Rotterdam, ZH, Netherlands; ³Manchester Royal Eye Hospital, Manchester, England, United Kingdom; ⁴Imagine Eyes, , France; ⁵Radboud universitair medisch centrum, Nijmegen, GE, Netherlands; ⁶Manchester Centre for Genomic Medicine, Manchester, England, United Kingdom

Disclosures: Danilo Andrade De Jesus: Code N (No Commercial Relationship) | David Green: Code N (No Commercial Relationship) | Darren Hargreaves: Code N (No Commercial Relationship) | Jane Gray: Code N (No Commercial Relationship) | Neda Shahedy: Code N (No Commercial Relationship) | Marine Durand: Imagine Eyes: Code E (Employment): None | Nicolas Chateau: Imagine Eyes: Code E (Employment): none | Sebastiaan Koninkx: Code N (No Commercial Relationship) | Pam Heutinck: Code N (No Commercial Relationship) | Kübra Liman: Code N (No Commercial Relationship) | Caroline C W Klaver: Code N (No Commercial Relationship) | Theo van Walsum: Code N (No Commercial Relationship) | Alberta Thiadens: Code N (No Commercial Relationship) | Panos Sergouniotis: Code N (No Commercial Relationship) | Luisa Sanchez Brea: Code N (No Commercial Relationship)

Purpose

This study aims to (1) establish novel image quality criteria for AO-FIO, ensuring consistency in protocol adherence, artifact assessment, and visualization of cone mosaic, (2) assess the variability introduced by image quality labelling, and (3) compare cone density in healthy controls between two cohorts.

Methods

The rtx1™ camera (Imagine Eyes, France) was used to acquire images from healthy controls following the AO-VISION protocol: 4° nasal to 12° temporal, -5° inferior to 5° superior (21 images, 4°x4° each, 2° overlap). Image quality was labelled by 5 experts as good, moderate, or poor based on: (1) protocol adherence, (2) presence of blurriness or artifacts, and (3) cone mosaic visualization (Fig.1). The Fleiss' Kappa was used to calculate the inter-grader agreement. The final image quality label was determined by majority voting. Cone density was estimated, using an in-house tool, within circular areas centered on the fovea, with the radius increasing in 1-degree steps. Comparisons were made between different image quality labels and cohorts.

Results

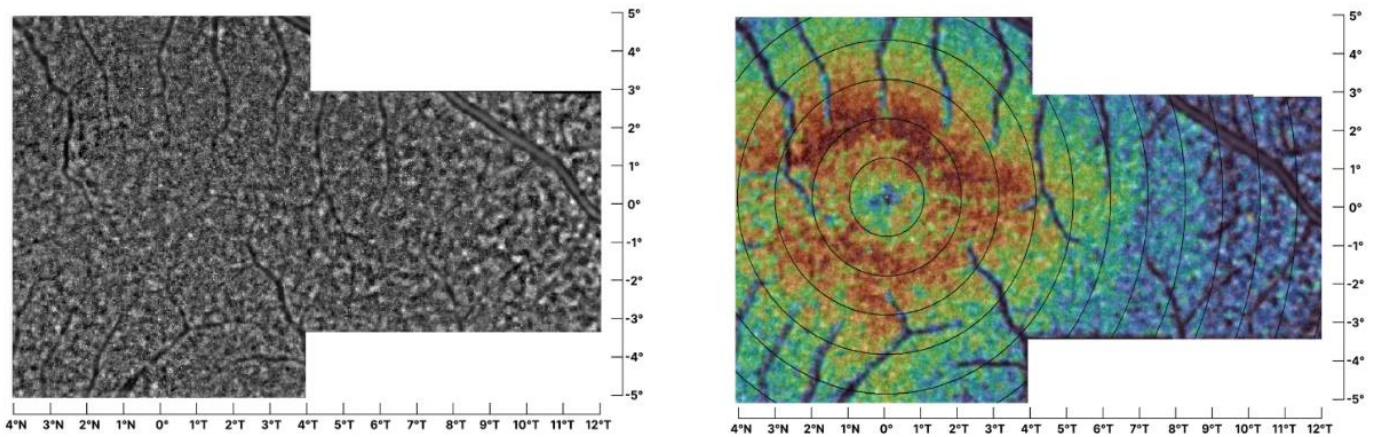
The study included 40 participants (29±10 years) at Erasmus MC (EMC) and 40 participants (42±18 years) at the University of Manchester (UM). The average agreement among graders for image quality labels was substantial and moderate, namely 0.63 and 0.57 for EMC and UM datasets, respectively. Majority voting set 14/17/9 and 16/16/8 images as good/moderate/poor for the EMC and UM datasets, respectively. Cone density measurements varied with image quality, with good montages producing consistently higher measurements compared to moderate and poor images (Fig.2). A significant statistical difference was observed between image quality groups ($p < 0.05$) for both datasets, at eccentricities up to 6 degrees ($p < 0.05$), and between cohorts ($p < 0.05$).

Conclusions

Cone density measurements are significantly influenced by image quality, with good-quality montages yielding more accurate results. These findings emphasize the critical role of standardized quality assessment in enhancing the reproducibility of AO-FIO studies and clinical practice usage.

Layman Abstract (optional): Provide a 50-200 word description of your work that non-scientists can understand. This study introduces new guidelines for assessing the quality of images taken with a special retinal imaging technique called Adaptive Optics Flood Illumination Ophthalmoscopy (AO-FIO), which helps doctors and researchers see tiny details of the retina. Experts graded the images as good, moderate, or poor based on how clear they were, whether they had any blurriness or artifacts, and how well they showed the retina's cone cells. The study found that higher quality images labelled as suggested in the guidelines gave more accurate and consistent measurements of these retina cells, which is important for both research and

medical use. By creating these new standards, the research aims to make retinal imaging more reliable and easier to use across different studies and clinical practice



AO-IQEval

Macro-analysis	Protocol adherence *	Good	No images are missing.
		Moderate	Minimal range is covered.
		Poor	Minimal range is not covered.
Macro-analysis	Blurriness and Artefacts #	Good	Blurriness or artefacts in < 10%.
		Moderate	Blurriness or artefacts in 10-50%.
		Poor	Blurriness or artefacts in > 50%.
Micro-analysis	Structure of Interest Visualization #	Good	Visible in > 90%.
		Moderate	Visible in 50-90%.
		Poor	Visible in <50%.
Overall	Good	All three criteria are "Good".	
	Moderate	None criteria is "Poor" (except for the Structure of Interest Visualization).	
	Poor	Protocol Adherence or Blurriness and Artefacts is "Poor".	

* The minimum range for this protocol is set from 3° nasal to 10° temporal and -3° to 3° vertically.

In case of doubt between Moderate and Poor (~50%), set as Moderate.

In-depth phenotypic study of a Novel Autosomal Dominant RPE65-related Retinal Dystrophy

Abstract 3122 - Poster B0158

Filip Van den Broeck*^{2,1}, **Eline Van Vooren**^{3,4}, **Manon Van Haute**¹, **Marieke De Bruyne**³, **Van De Sompele Stijn**³, **Mattias Van Heetvelde**^{3,4}, **Quinten Mahieu**^{3,4}, **Sheetal Uppal**⁵, **Eugenia Poliakov**⁵, **T. Michael Redmond**⁵, **Miriam Bauwens**^{3,4}, **Elfride De Baere**^{3,4}, **Julie De Zaeytijd**¹, **Bart Peter Leroy**^{1,2}

¹Department of Ophthalmology, Ghent University Hospital, Ghent, Belgium; ²Department of Head and Skin, Ghent University, Ghent, Belgium; ³Center for Medical Genetics, Ghent University Hospital, Ghent, Belgium; ⁴Department of Biomolecular Medicine, Ghent University, Ghent, Belgium; ⁵Laboratory of Retinal Cell and Molecular Biology, National Eye Institute, Bethesda, Maryland, United States;

Disclosures: Filip Van den Broeck: Code N (No Commercial Relationship) | Eline Van Vooren: Code N (No Commercial Relationship) | Manon Van Haute: Code N (No Commercial Relationship) | Marieke De Bruyne: Code N (No Commercial Relationship) | Van De Sompele Stijn: Code N (No Commercial Relationship) | Mattias Van Heetvelde: Code N (No Commercial Relationship) | Quinten Mahieu: Code N (No Commercial Relationship) | Sheetal Uppal: Code N (No Commercial Relationship) | Eugenia Poliakov: Code N (No Commercial Relationship) | T. Michael Redmond: Code N (No Commercial Relationship) | Miriam Bauwens: Code N (No Commercial Relationship) | Elfride De Baere: Code N (No Commercial Relationship) | Julie De Zaeytijd: Code N (No Commercial Relationship) | Bart Peter Leroy: Novartis: Code C (Consultant/Contractor): None; Spark Therapeutics: Code C (Consultant/Contractor): None; Novartis: Code F (Financial Support): None; Spark Therapeutics: Code F (Financial Support): None

Purpose

Variant p.(E519K) of *RPE65* was previously identified as the cause of an autosomal dominant (AD) retinal dystrophy in 15 Belgian families and in 20 isolated cases. A detailed phenotypic study of this novel macula-predominant dystrophy was performed through retrospective study of clinical data at a tertiary referral center for ophthalmic genetics (Ghent University Hospital, Ghent, Belgium).

Methods

A total of 125 eyes of 63 cases were retained after exclusion of eyes with comorbidity. Clinical data from deep phenotyping included a multigenerational pedigree, symptoms, psychophysical visual function testing and full-field flash electroretinography (ERG) as well as anatomical data including multimodal retinal imaging and adaptive-optics flood-illumination imaging.

Results

About fifty percent cases were asymptomatic but clinical signs were seen in all, with a median best-corrected visual acuity (BCVA) of 1.0 (range 0.8-1.0). Median age at symptom onset and BCVA was 57 years (range 24 - 76) and 0.8 (range 0.01-1.0, respectively, in symptomatic individuals). The main symptom was central visual loss. ERG in 29 cases indicated rod-predominant involvement in 56%, only rarely with additional cone involvement. In 25 cases short-wavelength autofluorescence imaging showed macular hypo-autofluorescent mottling often associated with limited hyperautofluorescent changes. In 26 cases a central pattern dystrophy almost indistinguishable from m.3243A>G-associated mitochondrial retinopathy was identified, with macular and peripapillary chorioretinal atrophy in many. Signs in the remaining cases are more aspecific but remain limited to the central retina. Foveal vitelliform lesions and cystoid macular oedema were uncommon findings, the former often associated with reduced BCVA. Disease severity relative to age was highly variable.

Conclusions

RPE65's p.(E519K) causes a completely penetrant, AD macula-predominant retinal dystrophy with rod-system involvement in about half of cases. Macular chorioretinal atrophy and vitelliform lesions was the main causes of vision loss. The cases with central hypo-autofluorescent mottling were most often asymptomatic with good BCVA. These phenotypes are distinct from those due to biallelic pathogenic variants and the p.(D477G) variant of *RPE65*. p.(E519K) constitutes an important differential diagnosis to be included in the work-up of inherited and acquired macula-predominant disorders.

Layman Abstract (optional): Provide a 50-200 word description of your work that non-scientists can understand. Describe the big picture and the implications of your findings, not the study itself and the associated details.

Our genome has two copies of the gene *RPE65* and contains the code for the production of a protein crucial in the recycling of the vitamin A-derivate upon which vision depends. Some individuals have a missing or anomalous copy, but this does not affect their retina nor their vision. When a child inherits two anomalous copies of this gene it will have a severe visual impairment from birth that progresses with age. Such inherited disease is said to show autosomal recessive inheritance in which 1 in 4 children will be affected. In 2011, it was discovered that a single anomalous copy of *RPE65* was the cause of an inherited retinal degeneration in an Irish family that was reminiscent of another inherited retinal condition caused by the gene *CHM*. Such a copy is said to be dominant with 1 in 2 probability of disease for each pregnancy. We recently discovered a second dominant copy in a large group of patients of Flemish descent who presented with an unexplained retinal disease that mainly affects the central area of vision and looks very different from the previously described diseases linked to *RPE65*. We describe the nature and the evolution of this novel inherited disease based on an analysis of the clinical and genetic data of a large patient cohort.

A two-year prospective natural history study of EYS-associated retinitis pigmentosa (KEYS study): assessment of progression using OCT and adaptive optics

Abstract 3135 - Poster B0171

Kiyoko Gocho^{*1,2}, **Masakazu Hiraoka**^{2,3}, **Satoshi Yokota**^{2,4}, **shohei kitahata**⁵, **Midori Yamamoto**², **Elena Gofas**^{2,6}, **YUKI TOGASHI**⁷, **Tomoko Kirihara**⁷, **Hisao Shimada**⁷, **Reza M. Haque**⁸, **Kate Grieve**⁶, **Michel Paques**¹, **Michiko Mandai**^{2,9}, **Yasuo Kurimoto**^{2,4}, **Akiko Maeda**^{2,9}

¹CIC1423 Inserm-DGOS, Hopital National des 15-20, Paris, Île-de-France, France; ²Kobe Shiritsu Kobe Eye Center Byoin, Kobe, Hyogo, Japan; ³Kawasaki Ika Daigaku, Kurashiki, Okayama, Japan; ⁴Kobe Shiritsu Iryo Center Chuo Shimin Byoin, Kobe, Hyogo, Japan; ⁵Yokohama Shiritsu Daigaku Fuzoku Shimin Sogo Iryo Center, Yokohama, Kanagawa, Japan; ⁶Institute de la Vision, Paris, France; ⁷Santen Seiyaku Kabushiki Kaisha, Osaka, Osaka, Japan; ⁸Santen Inc, Emeryville, California, United States; ⁹Ritsumeikan Daigaku, Kyoto, Japan

Disclosures: Kiyoko Gocho: Santen Pharmaceutical Co., Ltd.: Code F (Financial Support): none; Imagine eyes : Code O (Owner): spouse | Masakazu Hiraoka: Santen Pharmaceutical Co., Ltd.: Code F (Financial Support): none | Satoshi Yokota: Santen Pharmaceutical Co., Ltd.: Code F (Financial Support): none | shohei kitahata: Santen Pharmaceutical Co., Ltd.: Code F (Financial Support): none | Midori Yamamoto: Santen Pharmaceutical Co., Ltd.: Code F (Financial Support): none | Elena Gofas: Santen Pharmaceutical Co., Ltd.: Code F (Financial Support): none | YUKI TOGASHI: Santen Pharmaceutical Co., Ltd.: Code E (Employment): none | Tomoko Kirihara: Santen Pharmaceutical Co., Ltd.: Code E (Employment): none | Hisao Shimada: Santen Pharmaceutical Co., Ltd.: Code E (Employment): none | Reza M. Haque: Santen Pharmaceutical Co., Ltd.: Code E (Employment): none | Kate Grieve: Santen Pharmaceutical Co., Ltd.: Code F (Financial Support): none | Michel Paques: Santen Pharmaceutical Co., Ltd.: Code F (Financial Support): none | Michiko Mandai: Santen Pharmaceutical Co., Ltd.: Code F (Financial Support): none | Yasuo Kurimoto: Santen Pharmaceutical Co., Ltd.: Code F (Financial Support): none | Akiko Maeda: Santen Pharmaceutical Co., Ltd.: Code F (Financial Support): none

Purpose

The purpose of the Kobe EYS (KEYS) natural history study was to gain a better understanding of disease progression over time in subjects with EYS-associated retinitis pigmentosa (EYS-RP). Here we report on a sub-study aimed at comparing longitudinal assessments of cone photoreceptors using OCT and adaptive optics imaging over 2 years.

Methods

The retinas of 27 patients with EYSRP who visited Kobe Eye Hospital were examined every 6 months for 2 years using retinal OCT (Spectralis, Heidelberg Engineering, Germany) and an adaptive optics (AO) retinal camera (rtx1, Imagine Eyes, France). Ellipsoid zone width (EZW) and cone density (CD) were assessed at baseline and at each follow-up visit. EZW was measured in horizontal OCT B-scans by two graders. Cone density (CD) was assessed in AO images in 4 regions of interest (ROI) located on a central horizontal meridian at eccentricities of 2 and 4 degrees nasal and temporal. In each ROI, 2 graders annotated the cones visible in the AO image and the resulting cell coordinates were processed using the manufacturer's software to calculate local CD. Differences in EZW and CD between visits were analyzed by ANOVA.

Results

Subjects included 9 males and 18 females with a mean age of 44.0 ± 11.5 years. At baseline, horizontal EZW was $2053 \pm 1576 \mu\text{m}$ (mean \pm SD) and CD was 11156 ± 4331 , 9786 ± 3280 , 11514 ± 3385 and 10075 ± 2684 cell/ mm^2 (mean \pm SD) at 2N, 4N, 2T, 4T respectively. Analysis of longitudinal OCT results showed no statistically significant change in EZW between baseline and follow-up visits except for the last visit at 24 months. Analysis of AO results showed a significant reduction in CD at all visits, starting at the 6-month visit. The average rate of CD reduction over the 6-month periods was 10% at 2N and 2T, consistent with previous findings in RP.

Conclusions

Photoreceptor loss caused by RP progression could be detected and quantified with an AO camera in a 4-fold shorter time frame than that required for OCT. These findings demonstrate the value of AO imaging biomarkers in understanding the natural history of RP and evaluating the short-term efficacy of novel therapies.

Correlation Between Cone Density and Visual Function in 27 EYS-RP Patients Using AO Fundus Camera: A Subset Analysis of the KEYS Study

Abstract 3163 - Poster B0199

Masakazu Hiraoka*^{1,2}, **Akiko Maeda**^{1,3}, **Midori Yamamoto**¹, **Elena Gofas**^{1,5}, **shohei kitahata**⁹, **Satoshi Yokota**^{1,6}, **YUKI TOGASHI**⁷, **Tomoko Kiriara**⁷, **Hisao Shimada**⁸, **Reza M. Haque**⁸, **Yasuhiko Hiram**^{1,6}, **Yasuo Kurimoto**^{1,6}, **Kiyoko Gocho**^{1,4}

¹Kobe Shiritsu Kobe Eye Center Byoin, Kobe, Hyogo, Japan; ²Kawasaki Ika Daigaku, Kurashiki, Okayama, Japan; ³Ritsumeikan Daigaku, Kyoto, Kyoto, Japan; ⁴Hopital National des 15-20, Paris, Île-de-France, France; ⁵Institut de la vision, Paris, Île-de-France, France; ⁶Kobe Shiritsu Iryo Center Chuo Shimin Byoin, Kobe, Hyogo, Japan; ⁷Santen Seiyaku Kabushiki Kaisha, Osaka, Osaka, Japan; ⁸Santen Inc, Emeryville, California, United States; ⁹Yokohama Shiritsu Daigaku, Yokohama, Kanagawa, Japan

Disclosures: masakazu hiraoka: Santen Pharmaceutical Co.: Code F (Financial Support): None | Akiko Maeda: Santen Pharmaceutical Co.: Code F (Financial Support): None | Midori Yamamoto: Santen Pharmaceutical Co.: Code F (Financial Support): None | Elena Gofas: Santen Pharmaceutical Co.: Code F (Financial Support): None | shohei kitahata: Santen Pharmaceutical Co.: Code F (Financial Support): None | Satoshi Yokota: Santen Pharmaceutical Co.: Code F (Financial Support): None | YUKI TOGASHI: Santen Pharmaceutical Co.: Code E (Employment): None | Tomoko Kiriara: Santen Pharmaceutical Co.: Code E (Employment): None | Hisao Shimada: Santen Pharmaceutical Co.: Code E (Employment): None | Reza M. Haque: Santen Pharmaceutical Co.: Code E (Employment): None | Yasuhiko Hiram: Santen Pharmaceutical Co.: Code F (Financial Support): None | Yasuo Kurimoto: Santen Pharmaceutical Co.: Code F (Financial Support): None | Kiyoko Gocho: Santen Pharmaceutical Co.: Code F (Financial Support): None

Purpose

In Japan, approximately 20-30% of autosomal recessive retinitis pigmentosa (RP) cases are caused by EYS gene variants, making it a common genetic cause of RP in the Japanese population. Predicting disease progression in these patients is critical for effective management. Therefore, studies evaluating the longitudinal changes in cone density and visual function progression in EYS-related RP patients are needed. This study aimed to observe cone photoreceptor density (CD) over a two-year period in EYS-RP using an adaptive optics (AO) fundus camera and to investigate the correlation between CD, visual field test and visual acuity.

Methods

A total of 27 patients (27 eyes, 25 of right and 2 left eyes) with RP were enrolled in this study. Each patient underwent measurements of best-corrected decimal visual acuity (BCVA), AO imaging and the 10-2 test of Humphry visual fields analyzer (HFA). AO images centered on the fovea were obtained using an adaptive optics flood illuminated ophthalmoscope (rtx1™, Imagine Eyes, Orsay, France), with CD measured at 2 degrees and 4 degrees from the foveal center. Each ROI of AO data was analyzed and compared with BCVA and the mean deviation (MD) of HFA.

Results

The mean age of 27 subjects (9 males and 18 females) was 44.0 ± 11.5 years old. At baseline, CD was 11156 ± 4331 , 9786 ± 3280 , 11514 ± 3385 and 10075 ± 2684 cell/mm² (mean \pm SD) at 2N, 4N, 2T, 4T respectively, BCVA was 0.97 ± 0.38 (decimal) and MD was -15.5 ± 7.84 [YT1] dB. The correlation coefficient between MD and CD at 2 and 4 degrees were 0.002 and -0.2, respectively, while CD and visual acuity was 0.22 at 2 degrees and 0.21 at 4 degrees, indicating a weak correlation. The average rate of CD reduction of 6 months at 2N, 4N, 2T, 4T, were 9.8, 9.6, 7.6, 11.3%, respectively. AO imaging detected a sensitive decrease in cone density over six-month intervals in RP patients, while visual acuity and MD showed no significant changes over the two-year period.

Conclusions

AO imaging demonstrated a reduction in foveal cone density in RP patients over a two-year period. AO imaging may shorten the duration of observational studies by providing an early indication of RP progression rate.